

Pavlo Yevtushenko, Florian Hellmeier*, Jan Bruening, Titus Kuehne and Leonid Goubergrits

Numerical investigation of the impact of branching vessel boundary conditions on aortic hemodynamics

Abstract: CFD has gained significant attention as a tool to model aortic hemodynamics. However, obtaining accurate patient-specific boundary conditions still poses a major challenge and represents a major source of uncertainties, which are difficult to quantify. This study presents an attempt to quantify these uncertainties by comparing 14 patient-specific simulations of the aorta (reference method), each exhibiting stenosis, against simulations using the same geometries without the branching vessels of the aortic arch (simplified method).

Results were evaluated by comparing pressure drop along the aorta, secondary flow degree (SFD) and surface-averaged wall shear stress (WSS) for each patient. The comparison shows little difference in pressure drop between the two methods (simplified-reference) with the mean difference being 1.2 mmHg (standard deviation: 3.0 mmHg). SFD and WSS, however, show striking differences between the methods: SFD downstream of the stenosis is on average 61 % higher in the simplified cases, while WSS is on average 3.0 Pa lower in the simplified cases.

Although unphysiological, the comparison of both methods gives an upper bound for the error introduced by uncertainties in branching vessel boundary conditions. For the pressure drop this error appears to be remarkably low, while being unacceptably high for SFD and WSS.

Keywords: CFD, aortic hemodynamics, coarctation of the

aorta, modelling and simulation

<https://doi.org/10.1515/cdbme-2017-0066>

1 Introduction

Modelling aortic hemodynamics using CFD holds enormous potential to understand, predict and ultimately aid in the clinical decision making process [1,2]. Since the aorta is only a small part of the cardiovascular system, modelling its hemodynamics requires both in- and outflow boundary conditions. These, in turn, significantly affect the solution obtained within the domain [3,4] and are therefore critical for accurate calculations.

A common method for obtaining these boundary conditions in vivo is 4D MRI. While flow calculations with MRI-based velocity inflow conditions show good agreement with in vivo catheter measurements [5], obtaining reasonable boundary conditions for the aortic branches from 4D MRI is rather difficult for several reasons. The spatial resolution of most 4D MRI data sets is rather coarse compared to the branching vessel diameters, with some branching vessels being as small as 4 mm in this study. This results in poor resolution of the branching vessel flow by only a few voxels and thereby introduces large errors. Other complicating factors include vessel motion during the respiratory cycle and background noise.

To provide a quantitative assessment of the influence of branching vessel flow on simulated aortic hemodynamics, this study compares 14 reference cases with branching vessel flow distributed according to Murray's law with 14 corresponding cases omitting all three branching vessels, for a total of 28 patient-specific geometries, each suffering from aortic coarctation (CoA) downstream of the aortic arch.

Patients with CoA were chosen because they exhibit a significant pressure drop and thus provide an important parameter to compare. While the simplified cases are highly unphysiological, they represent the most extreme case of

*Corresponding author: **Florian Hellmeier:** Charité – Universitätsmedizin Berlin, Augustenburger Platz 1, 13353 Berlin, Germany, e-mail: florian.hellmeier@charite.de

Pavlo Yevtushenko, Jan Bruening, Leonid Goubergrits: Charité – Universitätsmedizin Berlin, Augustenburger Platz 1, 13353 Berlin, Germany, e-mail: yevtu@mailbox.tu-berlin.de, jan.bruening@charite.de, leonid.goubergrits@charite.de

Titus Kuehne: Deutsches Herzzentrum Berlin, Augustenburger Platz 1, 13353 Berlin, Germany, e-mail: titus.kuehne@dhzb.de

underestimating branching vessel flow and thus provide a lower bound for the error introduced by this kind of uncertainty.

2 Materials and methods

2.1 Patient data acquisition

For each patient, the aortic anatomy was captured using a whole-body Achieva 1.5 T MR scanner. The acquired 3D whole-heart data sets have a reconstructed spatial resolution of $0.66 \times 0.66 \times 1.6$ mm. Additionally, 4D VEC MRI data was used to obtain peak-systolic blood flow rates for each patient, which were then used to set in- and outlet boundary conditions. A detailed description of the acquisition method can be found in earlier studies [5].

2.2 Geometry and mesh generation

From the obtained 3D whole-heart data sets, 3D geometries of the aortas were reconstructed using ZIBAmira (Zuse Institute, Berlin, Germany) as described previously [1]. These geometries were used for the reference cases with branching vessels. The geometries for the simplified method were derived from the reference geometries by manually removing the aortic branches for each geometry using ReMESH (IMATI, Genoa, Italy). In total, 28 geometries were obtained, consisting of 14 original geometries with branching vessels and 14 modified geometries without branching vessels. Figure 1 shows all 14 non-modified geometries.

Fluid domain discretization was performed using ANSYS Gambit (ANSYS, Canonsburg, USA). Meshes were constructed from unstructured tetrahedral elements with a three-layer prismatic boundary layer at the vessel walls to capture near-wall flow accurately. Depending on aortic volume, the mesh element count varied from 1.0 to 2.7 million cells, with a mean cell volume of approximately 0.03 mm³ for all meshes. Again, a detailed description of the method as well as mesh quality requirements and a mesh independence study can be found in earlier studies [1].

2.3 Numerical setup

For comparability reasons, every case was performed with identical solver parameters and physical models, except for the patient-specific flow boundary conditions, which are

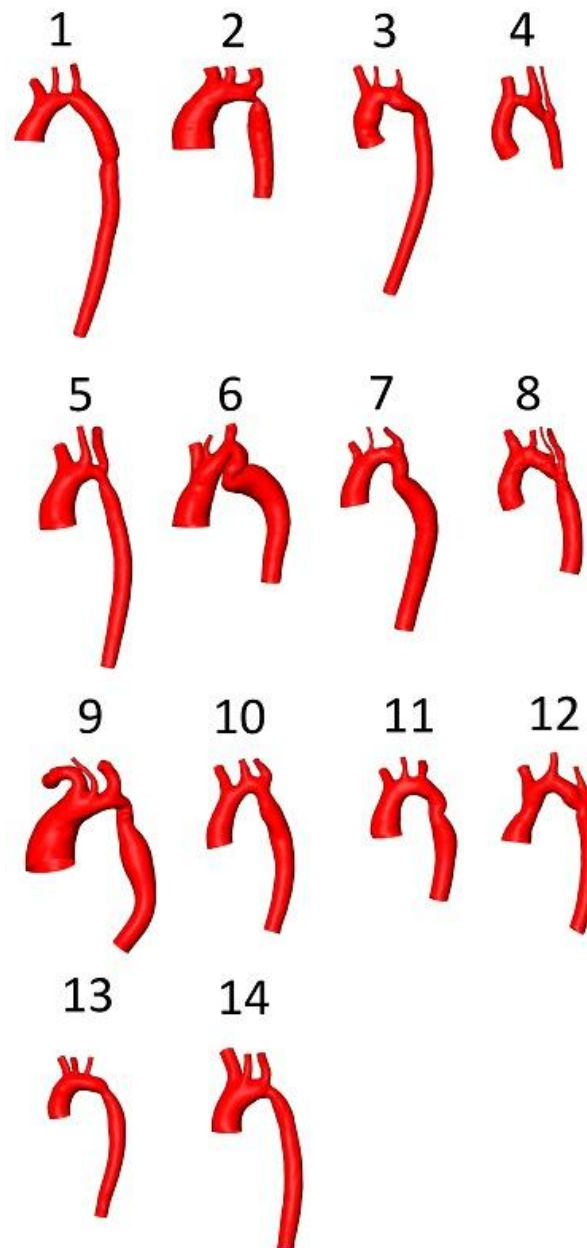


Figure 1: Aortic reference geometries with branching vessels.

discussed in the next paragraph. The solver package used was Fluent version 16 (ANSYS). Fluent's unsteady, pressure-based, incompressible solver with SIMPLEC pressure correction scheme was used to solve the mass and momentum conservation equations. For time discretisation, a second-order implicit time stepping method with a time step size of 1 ms was chosen. Turbulent effects were accounted for with a $k-\omega$ SST model. Furthermore, blood was assumed to be a non-Newtonian fluid and the viscosity was modelled using a custom shear stress-dependent viscosity model described earlier [6].

2.4 Boundary conditions

Volumetric flow rates were set at the inlet (aorta ascendens) and outlet (aorta descendens) of each geometry according to patient-specific 4D MRI data. The difference between aorta ascendens and descendens flow was distributed among the branching vessels according to Murray's law, which relates the flow rate to the third power of a vessel's hydraulic diameter.

For simplicity reasons, inlet flow was prescribed using a plug profile. Outlet flow was defined using Fluent's outflow boundary condition, which prescribes a constant mass-flow but leaves pressure and in-plane velocity open to calculation. Aorta ascendens and descendens flow rates for each patient are shown in table 1.

Table 1: Aorta ascendens and descendens boundary conditions.

patient	flow aorta ascendens [ml/s]	flow aorta descendens [ml/s]
1	360	160
2	260	110
3	410	280
4	350	130
5	480	160
6	330	110
7	300	110
8	350	80
9	560	270
10	650	300
11	510	230
12	460	300
13	250	150
14	310	170

For the simplified cases, in- and outflow have been set to the peak-systolic aorta descendens flow. This was done to obtain equal stenosis flow rates for reference and simplified cases, which was possible because the stenosis is located downstream of the branching vessels in all patients. Equal stenosis flow is important for pressure drop comparability, as most of the pressure drop occurs across the stenosis and is dependent on the flow rate through the stenosis.

3 Results

Please note that all differences between simplified and reference cases in this section are defined as $\Delta x = x_{\text{simplified}} - x_{\text{reference}}$. Pressures were evaluated along the aortic centerline. Total pressure drop (TPD), which is defined as the pressure difference between the beginning of the centerline and the end of the centerline, as well as the mean pointwise pressure difference (MPPD) along the centerline were compared. The pressure differences between the simplified and reference cases were generally small (mean Δ TPD: 1.20 mmHg, mean MPPD: -0.12 mmHg) with some patients exhibiting more pronounced differences, e.g. patient 3 (Δ TPD: 7.66 mmHg, MPPD: -5.89 mmHg). Detailed results are shown in table 2.

Secondary flow degree (SFD), defined as the ratio of mean in-plane to mean out-of-plane velocity, was evaluated at two cross-sections: one 1.5 cm upstream of the brachiocephalic artery (ascendens cross-section) and one 3 cm downstream of the stenosis (descendens cross-section). Both cross-sections were aligned to be perpendicular to the aortic centerline and, thus, the main flow direction. Additionally, SFD differences were normalized with the respective reference case SFD value to obtain a relative value for this rather abstract quantity. While the normalized SFD differences were mostly below 1, two patients stand out: patient 4 exhibited a normalized ascendens SFD difference (Δ SFD_{norm,asc}) of 3.45 and patient 8 exhibited a normalized descendens SFD difference (Δ SFD_{norm,des}) of 4.69. Again, detailed results are given in table 2.

The last parameter to be compared was wall shear stress (WSS), specifically the surface-averaged WSS over the whole vessel wall. For this parameter, large differences exist between the simplified and reference cases (mean difference in surface-averaged WSS: -3.0 Pa, standard deviation: 3.4 Pa). For patients 8 and 10 the difference between the simplified and reference case was particularly pronounced at -8.0 and -8.4 Pa, respectively. Detailed results are also shown in table 2.

Table 2: Pressure drop, WSS and SFD differences between simplified and reference cases ($\Delta x = x_{\text{simplified}} - x_{\text{reference}}$). MPPD is mean pointwise pressure difference and Δ TPD is total pressure drop difference. Δ WSS is the difference in surface-averaged WSS. Δ SFD_{norm,asc} and Δ SFD_{norm,des} are the differences in aorta ascendens and descendens SFD, normalized by the respective reference case SFD. Mean and SD denote the mean and standard deviation of the respective column.

patient	MPPD [mmHg]	Δ TPD [mmHg]	Δ WSS [Pa]	Δ SFD _{norm,asc}	Δ SFD _{norm,des}
1	1.26	-1.10	-4.1	0.13	0.30
2	-1.23	3.58	0.1	0.25	0.46
3	-5.89	7.66	2.3	0.54	0.54
4	4.05	-4.00	-6.5	3.45	0.97
5	-0.24	0.75	-4.7	0.22	0.41
6	0.19	1.01	-1.1	0.56	-0.29
7	-0.21	1.05	-2.4	0.07	1.48
8	0.23	0.32	-8.0	0.02	4.69
9	-0.61	1.39	-1.1	0.10	-0.04
10	3.62	-1.09	-8.4	0.12	0.21
11	1.03	0.63	-6.8	0.19	-0.09
12	2.72	-1.83	-2.1	0.05	-0.28
13	-3.09	3.69	-0.4	0.17	-0.10
14	-3.57	4.77	0.6	0.09	0.26
mean	-0.12	1.20	-3.0	0.43	0.61
SD	2.75	2.97	3.4	0.89	1.27

4 Conclusion

As expected, comparison of the simplified cases with the reference cases showed differences in pressure drop, SFD and WSS.

The smallest differences were observed for the pressure drop, being as low as few mmHg for most cases. Although most of the pressure drop in a stenosed aorta is expected to occur in the stenosis, this is still surprising, especially compared to the SFD results.

SFD, which is an indicator for basic flow structure, differs remarkably for all cases, indicating a high sensitivity of flow structure to branching vessel flow. The direction of these differences also reveals interesting information: since most of these differences are positive, meaning the reference cases exhibit less swirling flows, the branching vessels appear to have stabilizing effect on aortic flow. The pressure drop across the stenosis however seems largely unaffected by this, as seen from the pressure differences.

Surface-averaged WSS values also differ remarkably between simplified and reference simulations, indirectly

supporting the notion of flow structure sensitivity to branching vessel flow.

Overall, branching vessel flow does have a non-negligible impact on aortic flow. However, considering that the simplified cases completely omit branching vessel flow, these differences appear not to be as striking as one would expect. Particularly pressure drop seems rather insensitive to branching vessel flow. Pressure drop calculation can therefore be reliable, even with high branching vessel flow uncertainties. If particular flow features, such as helicity or backflow, are of interest, care must be taken to obtain reasonably accurate branching vessel boundary conditions, as these can significantly alter the flow structure.

Authors' Statement:

Research funding: The work was partially funded by the Deutsche Forschungsgemeinschaft (grant ID: GO 1067/6-1).

Conflict of interest: The authors state no conflict of interest.

Informed consent: Informed consent has been obtained from all individuals included in this study. Ethical approval: The research related to human use complies with all relevant national regulations, institutional policies and was performed in accordance with the tenets of the Helsinki Declaration, and has been approved by the authors' institutional review board or equivalent committee.

References

- [1] Goubergrits L, Mevert R, Yevtushenko P, et al. The impact of MRI-based inflow for the hemodynamic evaluation of aortic coarctation. *Ann Biomed Eng* 2013; 41:2575-2587.
- [2] Alimohammadi M, Sherwood JM, Karimpour M, Agu O, Balabani S, Díaz-Zuccarini V. Aortic dissection simulation models for clinical support: fluid-structure interaction vs. rigid wall models. *Biomed Eng Online* 2015; 14:34; doi: 10.1186/s12938-015-0032-6.
- [3] Gallo D, De Santis G, Negri F, et al. On the use of in vivo measured flow rates as boundary conditions for image-based hemodynamic models of the human aorta: implications for indicators of abnormal flow. *Ann Biomed Eng* 2012; 40:729-741.
- [4] Morbiducci U, Ponzini R, Gallo D, Bignardi C, Rizzo G. Inflow boundary conditions for image-based computational hemodynamics: impact of idealized versus measured velocity profiles in the human aorta. *J Biomech* 2013; 46:102-109.
- [5] Goubergrits L, Riesenkampff E, Yevtushenko P, et al. MRI-based computational fluid dynamics for diagnosis and treatment prediction: clinical validation study in patients with coarctation of aorta. *J Magn Reson Imaging* 2015; 41:909-916
- [6] Wellnhofer E, Osman J, Kertzscher U, Affeld K, Fleck E, Goubergrits L. Flow simulation studies in coronary arteries—impact of side-branches. *Atherosclerosis* 2010; 213:475-481